Impedance of space-charge-limited currents in organic light-emitting diodes with double injection and strong recombination

Ángeles Pitarch, Germà Garcia-Belmonte, and Juan Bisquert[a)]
Departament de Ciències Experimentals, Universitat Jaume I, 12071 Castelló, Spain

Henk J. Bolink
Institut de Ciència Molecular, Universitat de València, Poligon La Coma s/n, 46980 Paterna, València, Spain

(Received 14 April 2006; accepted 17 June 2006; published online 18 October 2006)

The impedance model for a one-carrier space-charge-limited (SCL) current has been applied to explain some experimental features of double carrier organic light-emitting diodes. We report the analytical model of impedance of bipolar drift transport in SCL regime in the limit of infinite recombination. In this limit the ac impedance function is identical to that of a single carrier device, with a transit time modified by the sum of mobilities for electrons and holes, $\mu_n+\mu_p$. The static capacitance $C(\omega\rightarrow 0)$ is a factor of $\frac{3}{4}$ lower than the geometric capacitance, as observed for single carrier devices, but it is shifted to higher frequencies. It follows that impedance measurements in the dual-carrier organic diodes with strong recombination provide the combination of $\mu_n+\mu_p$. For the mobilities of the different carriers to be determined separately, additional information is required.
 [DOI: 10.1063/1.2358302]

I. INTRODUCTION

Since the discovery of electroluminescence in polymers,[1] the study and understanding of optical and electronic properties of organic light-emitting diodes (OLEDs) have received considerable attention. Their potential for low cost manufacturing and mechanical flexibility makes these materials promising for many display applications.

In order to optimize the device efficiency of OLEDs a balanced distribution of the injected carriers is required. Impedance spectroscopy is a powerful tool to investigate the charge transport and relaxation processes in solid state devices. By means of this technique one can discern the different processes that occur on different time scales and get extended information about the carrier and field distributions inside the OLED. Several studies of impedance spectroscopy were interpreted with models for one-carrier space-charge-limited current[2,3] (SCLC) to explain some features in OLEDs.[4–9] Although useful to explain the phenomena observed in hole only devices, it has limited use for emitting, thus double carrier, devices. Therefore, it is of great interest to have a model capable of describing the experimental phenomena observed for double carrier light-emitting displays.

General ac impedance models of bipolar devices with arbitrary recombination, constitute a complex problem due to partial neutralization of the space charge if restricted recombination permits the coexistence of electrons and holes in extended regions of the organic layer. In this paper we present a model that provides a significant step towards a general understanding of ac impedance of OLEDs under normal light-emitting conditions. The assumption that there exists a large recombination rate simplifies the problem because carrier distributions completely separate in n and p regions that meet at the recombination plane. Such an assumption is realistic for a number of experimental OLEDs, as it has been reported that a rather narrow recombination zone exists.[10] Here we derive and discuss the impedance model of double injection SCLC in this case. We give an equivalent circuit explaining the impedance spectra at the low frequency limit for two-carrier devices[11] and compare it with the case of one-carrier device. There have been attemps to derive the minority carrier mobility from ac impedance using two-carrier models.[5,11] However, Poplavskyy and So[10] have reported evidence that the space-charge-related impedance response of dual-carrier diodes is dominated by combined electron-hole response, as proposed in the theory presented below.

In the next section we revise the characteristics of both dc and ac characteristics in single-carrier devices. In Sec. III we solve the model for double injection in the frequency domain in order to determine an analytical expression for the impedance.

II. SINGLE CARRIER MODEL

Single carrier devices, formed by using external contacts that allow only the injection of one type of carrier, are useful to investigate the transport properties of organic semiconductors. The ac impedance model for SCLC regime of a single carrier is well known.[2,3] The basic equations describing electron transport and distribution are the current-flow equation for carrier drift and the Poisson equation,

$$J_0 = e\mu nE, \tag{1}$$

[a)]Author to whom correspondence should be addressed; electronic mail: bisquert@uji.es

$$\frac{\varepsilon}{e}\frac{dE}{dx} = -n, \tag{2}$$

where μ is the drift mobility, which is assumed constant, n is the electron carrier density, e is the elementary charge, J_0 is the steady-state current density, which is constant across the sample, ε is the dielectric constant, and E is the electric field intensity. The solution of the above equations with boundary condition $E=0$ at the cathode is given by the Mott-Gurney square-law equation,

$$J_0 = \frac{9}{8}\varepsilon\mu\frac{V_0^2}{L^3}, \tag{3}$$

where V_0 the voltage across the organic layer.

In order to treat the time-dependent situation, we add the displacement current in the current-flow equation,

$$J = e\mu nE + \varepsilon\frac{\partial E}{\partial t}. \tag{4}$$

The impedance measurement corresponds to a small sinusoidal perturbation over a steady state. We separate the steady-state and modulated contributions by defining $E(x,t)=E_0(x)+E_1(x,t)$, $V(x,t)=V_0(x)+V_1(x,t)$, $J(x,t)=J_0(x)+J_1(x,t)$, and $n(x,t)=n_0(x)+n_1(x,t)$. From the solution of the above equations the ac impedance is given as[2,12]

$$Z(\omega) = \frac{6}{g_0(i\omega\tau)^3}\left[1 - i\omega\tau + \frac{1}{2}(i\omega\tau)^2 - e^{-i\omega\tau}\right]. \tag{5}$$

Expanding the exponential terms, we obtain the low frequency limit of the admittance,

$$Y = g_0 + i\omega\frac{g_0\tau}{4}, \tag{6}$$

with the low frequency conductance

$$g_0 = \frac{dJ_0}{dV_0} = \frac{9}{4}\varepsilon\mu\frac{V_0}{L^3} \tag{7}$$

and the transit time

$$\tau = \frac{4}{3}\frac{L^2}{\mu V_0}. \tag{8}$$

The admittance in Eq. (6) represents a capacitance

$$C' = \frac{3}{4}C_g, \tag{9}$$

where $C_g=\varepsilon/L$ is the geometric capacitance and resistance $R=g_0^{-1}$ in parallel, as shown in Fig. 1(a). The high frequency limit for the complex admittance is

$$Y = \frac{2g_0}{3} + i\omega C_g, \tag{10}$$

which represents the same equivalent circuit with different parameters.

III. TWO-CARRIER MODEL

In the model for two carriers, we consider the OLED as an insulator with double injection through Ohmic injecting contacts, free both of traps, and thermally free carriers. In this approximation we ignore the injection barriers. In the best working OLEDs under normal driving conditions this approximation is valid as the onset of light emission is close to the photonic gap. Electrons are injected in the conduction band at the cathode and holes are injected in the valence band at the anode, and both of them drift to the plane of recombination at x_p, where they meet and recombine. We consider an infinite recombination rate, therefore on the anode side ($0 \leqslant x \leqslant x_p$) there are only holes and current is a pure hole current. Similarly, on the cathode side ($x_p \leqslant x \leqslant L$) we have only electrons, and thus the current is purely based on electrons.

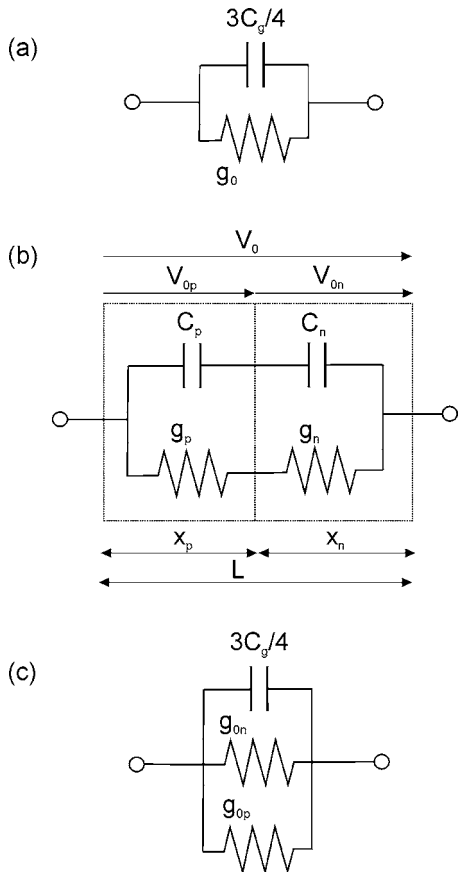

FIG. 1. Equivalent circuits of impedance models discussed in this work. (a) Low frequency limit of one-carrier device model. (b) Low frequency limit for two-carrier device model, indicating spatial and potential distributions of n and p regions. (c) Alternative representation of low frequency limit for two-carrier device model.

The equations characterizing double injection into a perfect insulator are the current-flow equation and the Poisson equation, similar as in the case of the one-carrier model. In the hole region, they are

$$J_0 = J_{0p} = e\mu_p pE, \tag{11}$$

$$\frac{\varepsilon}{e}\frac{dE}{dx} = p. \tag{12}$$

Similarly, in the electron region,

$$J_0 = J_{0n} = e\mu_n nE, \tag{13}$$

$$\frac{\varepsilon}{e}\frac{dE}{dx} = -n, \tag{14}$$

where μ_n and μ_p are the electron and hole drift mobility, respectively, n and p the free electron and hole densities, respectively, and J_{0p} and J_{0n} the hole and electron steady-state current density, respectively, both of them being constant across their corresponding region.

The solutions in both regions are tied together by continuity of the E field in the recombination plane,

$$E_p(x_p) = E_n(x_p), \tag{15}$$

where

$$E_p(x_p) = -\frac{3}{2}\frac{V_{0p}}{x_p}, \quad E_n(x_p) = -\frac{3}{2}\frac{V_{0n}}{x_n}. \tag{16}$$

From the last boundary condition, we derive the useful next relations,

$$\frac{V_{0p}}{x_p} = \frac{V_{0n}}{x_n}, \tag{17}$$

$$x_p = \frac{\mu_p}{\mu_p + \mu_n}L. \tag{18}$$

The steady-state solution of the above equation [Eqs. (11)–(14)] is given by the Mott-Gurney law in both regions,

$$J_{0p} = \frac{9}{8}\varepsilon\mu_p\frac{V_{0p}^2}{x_p^3}, \quad J_{0n} = \frac{9}{8}\varepsilon\mu_n\frac{V_{0n}^2}{x_n^3}, \tag{19}$$

with V_{0p} and V_{0n} the voltage in the hole and electron regions, respectively, and x_p and x_n the width of each region. By means of Eqs. (17) and (18) and the fact that $V_0 = V_{0p} + V_{0n}$, we can give the potential drop in both regions as a function of mobilities and V_0:

$$V_{0p} = V_0\frac{\mu_p}{\mu_n + \mu_p}, \tag{20}$$

$$V_{0n} = V_0\frac{\mu_n}{\mu_n + \mu_p}. \tag{21}$$

Using these relationships, we obtain the J-V characteristic in a simple form,[13]

$$J_0 = \frac{9}{8}\varepsilon(\mu_n + \mu_p)\frac{V_0^2}{L^3}. \tag{22}$$

It means that the total current density can be viewed as the sum of two SCL currents which traverse the entire sample independent of each other.

The strength of the electrical field increases from both contacts (where $E=0$) towards the recombination plane, whose position is determined by the carrier mobilities, as stated in Eq. (18). Accordingly the concentration of electrons and holes decreases, respectively, from the cathode and anode towards the recombination plane, as shown in Fig. 2.[14] In the case of low electron mobility, holes reach the cathode before electrons can leave it. As electron mobility increases, recombination plane shifts to the anode. When carrier mobilities are equal, electrons and holes recombine in the center of the film.

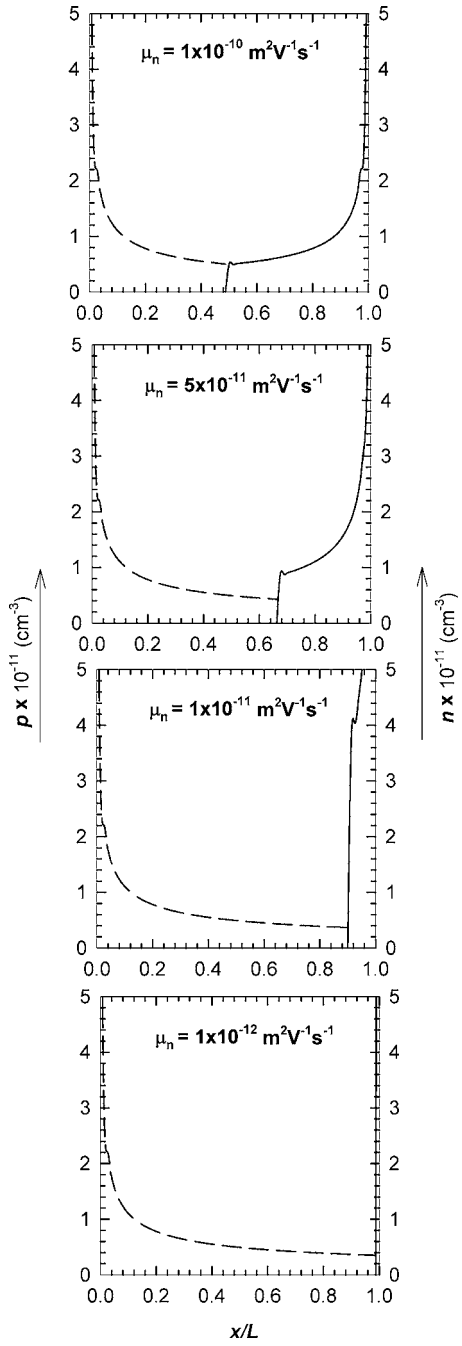

FIG. 2. Simulations of the electron (n) and hole (p) carrier distributions in a bipolar device with drift transport and infinite recombination. Parameters $\varepsilon = 10^{-12}$ F/m, $j = 5\times10^{-8}$ A/m^2, $L = 80$ nm, $\mu_p = 10^{-10}$ m^2 V^{-1} s^{-1}, and electron mobilities, as indicated.

Next we solve the drift-Poisson equations in the frequency domain by adding the displacement current like in the case of one carrier and proceeding in the same way. The steady-state and time-dependent contributions are separated similarly as in the previous case. The two transport regions are linked by continuity of electrical field and potential at the recombination plane. The solution provides us an analytical expression for the frequency dependent impedance,

$$Z(\omega)=\frac{6}{g_p(i\omega\tau_p)^3}\left[1-i\omega\tau_p+\frac{1}{2}(i\omega\tau_p)^2-e^{-i\omega\tau_p}\right]+\frac{6}{g_n(i\omega\tau_n)^3}\left[1-i\omega\tau_n+\frac{1}{2}(i\omega\tau_n)^2-e^{-i\omega\tau_n}\right], \quad (23)$$

where

$$g_p=\frac{9}{4}\varepsilon\mu_p\frac{V_{0p}}{x_p^3}, \quad g_n=\frac{9}{4}\varepsilon\mu_n\frac{V_{0n}}{(L-x_p)^3} \quad (24)$$

$$\tau_p=\frac{4}{3}\frac{x_p^2}{\mu_p V_{0p}}, \quad \tau_n=\frac{4}{3}\frac{x_n^2}{\mu_n V_{0n}}. \quad (25)$$

Equation (23) corresponds to two impedances in series under SCLC regime, one for the hole region and the other one to the electron region. This is a logical result because $V_0=V_{0p}+V_{0n}$ and the current is constant across the sample. Using the Eqs. (18), (20), and (21), it is found that the separate transit times τ_p and τ_n have the same value:

$$\tau_n=\tau_p\equiv\tau_{np}=\frac{4}{3}\frac{L^2}{(\mu_p+\mu_n)V_0}. \quad (26)$$

It should be remarked that the transit time in two-carrier devices is always shorter than the transit time of a one-carrier device with the same length, since each carrier has to travel a shorter path. The low frequency limit of the admittance takes the form

$$Y=g_t+i\omega\frac{g_t^2}{4}\left(\frac{\tau_p}{g_p}+\frac{\tau_n}{g_n}\right), \quad (27)$$

where

$$g_t=(g_n^{-1}+g_p^{-1})^{-1}=\frac{dJ_0}{dV_0}=\frac{9}{4}\varepsilon(\mu_n+\mu_p)\frac{V_0}{L_3}. \quad (28)$$

That is, g_t corresponds to two resistances in series, each one describing one different region (hole and electron region, respectively). The complete impedance expression of Eq. (23) can be given in a simplified form,

$$Z(\omega)=\frac{6}{g_t(i\omega\tau_{np})^3}\left[1-i\omega\tau_{np}+\frac{1}{2}(i\omega\tau_{np})^2-e^{-i\omega\tau_{np}}\right]. \quad (29)$$

At low frequencies the capacitance reaches a frequency independent value.

$$C'=\frac{g_t^2}{4}\left(\frac{\tau_p}{g_p}+\frac{\tau_n}{g_n}\right). \quad (30)$$

Equation (30) can be expressed as two capacitances in series, each one corresponding to one different region (holes or electron region),

$$\frac{1}{C'}=\frac{1}{C_n}+\frac{1}{C_p}, \quad (31)$$

where

$$C_p=\frac{3}{4}\frac{\varepsilon}{x_p}, \quad C_n=\frac{3}{4}\frac{\varepsilon}{x_n}. \quad (32)$$

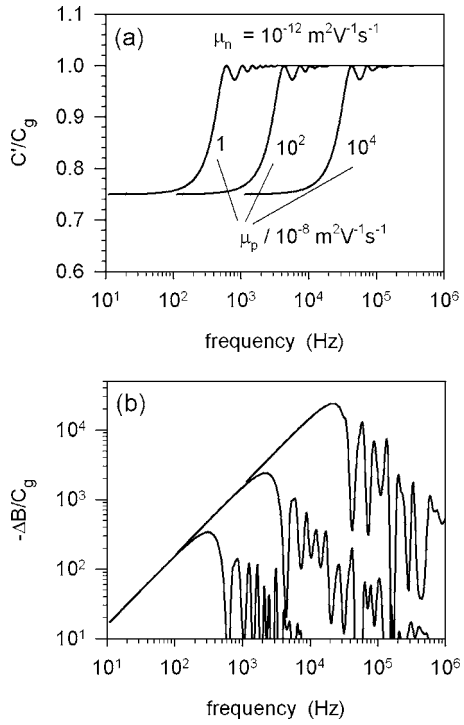

FIG. 3. (a) Simulations of capacitance spectra for different hole carrier mobilities, as indicated. (b) Same data as in (a) in terms of the change of susceptance. Parameters: $\varepsilon=2.7\times10^{-12}$ F/m, $j=10^{-2}$ A/m^2, and $L=80$ nm.

Finally, we obtain the simplified form of C',

$$C'=\frac{3}{4}\frac{\varepsilon}{L}, \quad (33)$$

It means that the low frequency capacitance is identical to that for the one-carrier case and, consequently, is independent of the features of the n and p regions. As expected, the equivalent circuit for low frequency admittance corresponds to two equivalent circuits bounded together in series, each of them describing the low frequency limit for the hole and electron regions respectively [see Fig. 1(b)].

It is also possible to represent the impedance at the low frequency limit in another way. Note that g_t^{-1} represents two resistances in parallel as shown in Fig. 1(c),

$$g_t=g_{0p}+g_{0n}, \quad (34)$$

each one being the resistance of the one-carrier model across the whole sample thickness for holes and electrons, respectively,

$$g_{0p}=\frac{9}{4}\varepsilon\mu_p\frac{V_0}{L^3}, \quad g_{0n}=\frac{9}{4}\varepsilon\mu_n\frac{V_0}{L^3}. \quad (35)$$

Figure 3(a) illustrates the frequency dependence of the capacitance, $C'(\omega)=\mathrm{Re}[1/i\omega Z(\omega)]$, according to Eq. (29), showing the transition of the capacitance from the geometrical value at high frequencies to Eq. (33) at low frequencies. We show the capacitance spectra for different mobilities in order to compare the shift to higher frequencies when the mobility increases. Figure 3(b) shows the same data in terms of the change of susceptance, $-\Delta B(\omega)=-\omega[C'(\omega)-C_g]$, that peaks at a frequency $f_{\max}$, which relates with the transit time

τ_{np} according to an approximate relation $\tau_{np} \approx 0.72 f_{\max}^{-1}$.[5] Here the shift of the transit time is more clearly appreciated in the displacement of the major peak.

It is obvious that the impedance and capacitance of two-carrier devices are formally the same as the impedance of one-carrier device in Eq. (5) but with a different apparent mobility ($\mu_p + \mu_n$ instead of μ), and as a consequence the spectra are shifted to higher frequencies. This shift is due to a lower characteristic time in the case of two-carrier devices, which relates to the fact that carriers in two-carrier devices have to traverse a shorter way (equivalent to the distance required to recombine with the opposite charge carrier). These results imply that the mobilities of the different carriers cannot be separated from impedance measurements in the dual-carrier diodes with strong recombination, as discussed in Ref. 10. Therefore, the analysis of double carrier, working, OLEDs using impedance spectroscopy is by itself not suitable for the determination of the individual carrier mobility. Nonetheless the sum of mobilities may constitute a valuable piece of information in combination with other measurements. For example, by combining impedance analysis of hole-only and double-injection devices with equal polymer active layer thickness, one could have access to the electron mobility by simple subtraction $\mu_n = \mu - \mu_p$. In practice this approach may encounter additional problems as the low frequency impedance usually measured yields more featured responses than the ideal expression derived here. The low frequency limit of the capacitance is reported to exhibit either positive values in excess of the geometric capacitance or negative (induction) responses.[9,15]

IV. CONCLUSION

The impedance model for double carrier SCLC in OLEDs has been derived using the assumption of a large recombination rate. In this case the impedance is readily calculated as the series combination of two SCLC transport layers. The equivalent circuit at low frequencies corresponds to two equivalent circuits bounded together in series, each of them describing the low frequency limit for hole and electron regions, respectively. The analytical expression for impedance of two-carrier devices reduces to the same analytical expression of one-carrier device, but $\mu_p + \mu_n$ instead of μ, and a shift to higher frequencies in the capacitance spectra.

ACKNOWLEDGMENTS

This work was supported by Generalitat Valenciana and Fundació Caixa Castelló-Bancaixa under Project No. P1 1B2005-12. One of the authors (H.B.) acknowledges the support of the Program "Ramon y Cajal" of the Spanish Ministry of Education and Science.

[1] J. H. Burroughes, D. D. C. Bradley, A. R. Brown, R. N. Marks, K. MacKay, R. H. Friend, P. L. Burn, and A. B. Holmes, Nature (London) **347**, 539 (1990).
[2] J. Shao and G. T. Wright, Solid-State Electron. **3**, 291 (1961).
[3] R. Kassing, Phys. Status Solidi A **28**, 107 (1975).
[4] H. C. F. Martens, H. B. Brom, and P. W. M. Blom, Phys. Rev. B **60**, R8489 (1999).
[5] H. C. F. Martens, J. N. Huiberts, and P. W. M. Blom, Appl. Phys. Lett. **77**, 1852 (2000).
[6] H. C. F. Martens, W. F. Pasveer, H. B. Brom, J. N. Huiberts, and P. W. M. Blom, Phys. Rev. B **63**, 125328 (2001).
[7] H. C. F. Martens, H. B. Brom, P. W. M. Blom, J. N. Huiberts, and H. F. M. Schoo, Synth. Met. **121**, 1643 (2001).
[8] S. Berleb and W. Brütting, Phys. Rev. Lett. **89**, 286601 (2002).
[9] H. H. P. Gommans, M. Kemerink, G. G. Andersson, and R. M. T. Pijper, Phys. Rev. B **69**, 155216 (2004).
[10] D. Poplavskyy and F. So, J. Appl. Phys. **99**, 033707 (2005).
[11] H. H. P. Gommans, M. Kemerink, and R. A. J. Janssen, Phys. Rev. B **72**, 235204 (2005).
[12] A. van der Ziel, *Solid State Physical Electronics* (Prentice-Hall, Englewood Cliffs, NJ, 1976).
[13] M. A. Lampert and P. Mark, *Current Injection in Solids* (Academic, New York, 1970).
[14] A. Pitarch, G. Garcia-Belmonte, and J. Bisquert, Proc. SPIE **5519**, 304 (2004).
[15] J. Bisquert, G. Garcia-Belmonte, A. Pitarch, and H. Bolink, Chem. Phys. Lett. **422**, 184 (2006).